ЭЛЕКТРОНИКА

UDC 541.124.2

PHYSICAL CHARACTERIZATION OF FERROELECTRIC THIN FILMS

V.V. Buniatyan, Mohammad Ali Khalili Araghi, A.A. Davtyan

National Polytechnic University of Armenia

Mg-doped $Ba_{0.8}Sr_{0.2}Mg_{0.1}Ti_{0.9}O_3$ (BST) thin film structural and physical characterization results are presented. The (Ba,Sr)<Mg>TiO_3 ceramic targets have been prepared by self-propagating high-temperature synthesis method and a nano-film is fabricated by the pulsed laser deposition method. Ferroelectric films have been physically characterized (thickness, surface morphology, composition) by means of ellipsometry, scanning-electron microscopy, Rutherford backscattering spectrometry (RBS) and atomic force microscopy (AFM) methods. The results of ellipsometric investigation of the Mg-doped $Ba_{0.8}Sr_{0.2}Mg_{0.1}Ti_{0.9}O_3$ thin film and the comparison of Mg-doped $Ba_{0.8}Sr_{0.2}Mg_{0.1}Ti_{0.9}O_3$ targets prepared by the SHS technology show that BST thin films behave differently than bulk BST. It is observed that the dielectric constant decreases with a decrease in the thickness of the BST thin film. The thickness dependence of the dielectric constant varies with the substrate temperature and the grain size effect. The thickness dependence of dielectric permittivity is explained in Schottky barrier model. The RBS investigations of the examined BST films confirm a stoichiometric growth and an excellent crystalline quality and confirm a stoichiometric good growth. The measured root mean square (rms) roughness is about 7,6 *nm*. The micrographs show a closed BST thin film without micro-cracks or pores. The BST surface possesses a grainy texture with a typical grain size of ~50 *nm*.

Keywords: barium-strontium titanate, ellipsometry, atomic force microscopy.

Introduction. Ferroelectric materials are very promising for a variety of applications such as high permittivity capacitors, ferroelectric memories, tunable microwave devices, pyroelectric sensors, piezoelectric transducers, electro -optic devices and PTC thermistors, as well as bio(chemical) sensors [1-3]. This wide range of applications is mainly attributed to the phase transitions in ferroelectrics. Ferroelectric materials tend to become paraelectric beyond a transition temperature called Curie temperature T_c. At the Curie temperature, the ferroelectric materials undergo a structural change from ferroelectric to paraelectric attaining highest dielectric constant. The ferroelectric characteristics like the composition-dependent Curie temperature and the electric field dependent dielectric permittivity have found applications in tunable fil-

ters, phase shifters and tunable antennas [1,2,4]. Due to the presence of oxygen vacancies and ionic conductance, perovskite oxides have a high catalytic activity to oxygen reduction and oxidation, and thus suitable for a large variety of sensor applications: magnetic sensors, pyroelectric detectors, optical memories and electro-optic modulators [3], microwave capacitors [1,2,4,5], solid-oxide fuel cells (SOFC)[6], as a sensing material in oxygen [7], carbon monoxide, hydrocarbon[8], nitrite oxide [9], humidity [10], ethanol [11], hydrogen peroxide [12], pH [13] and other bio(chemical) sensors.

$Ba_xSr_{1-x}TiO_3$ is the most commonly investigated material, since it has the highest dielectric constant at room temperature. It has been reported that [1,2,4,14-16] the main dielectric and catalytic properties of the ferroelectric materials strongly depend on the method of fabrication, structure and grain size, as well as on its composition, so controllable preparation of crystalline size and thin film has been focused in order to improve the device capability. For example, the grain size profoundly affects the dielectric properties of the BST thin films. The grain size decreases and grain boundary increases, as the thickness of the film reduces. Hence a thinner film has a higher leakage current density and a lower dielectric constant as compared to the thicker films [1,2,4]. It has been reported that the increased dielectric constant and the increased temperature variation is observed with an increased grain size by varying the oxygen pressure during sputtering. The thickness dependence of the dielectric constant varies with the substrate temperature and the grain size effect. In order to improve the performance of the BST-based different circuit elements, microwave capacitors, PTC resistors, ferroelectric memories, as well as sensors and actuators, the researchers extensively studied the BST ceramics and thin films doped by different rare earth materials. The use of isovalent dopants, such as strontium, have been used to move the Curie point to the optimal location for the desired application. From an application perspective, it is important to reduce the dependence of the relative dielectric constant on temperature. One significant advantage of ceramic and thin film ferroelectrics is the ease with which their properties can be adjusted by slight changes to the composition.

The effect of Mg doping on the BST ceramics and thin films was investigated previously in many works [14-16]. However, the Mg - doped BST ceramics in these studies were manly prepared by sintering the mixture of as-received BST and Mg-based chemical. It has been reported that Mg doping or MgO addition could be used in BST ceramics and thin films to suppress the permittivity and losses [14].

In this connection, the goal of this work is to investigate the structural and physical characteristics of Mg-doped $Ba_{0.8}Sr_{0.2}Mg_{0.1}Ti_{0.9}O_3$ thin films, obtained by the pulsed laser deposition (PLD) technique.

Perovskite-oxide targets of Mg-doped $Ba_{0.8}Sr_{0.2}Mg_{0.1}Ti_{0.9}O_3$ are prepared by SHS technology [17] and thin films (~100 *nm* thick) were prepared onto a *Si-SiO*$_2$ substrates (*p-Si*, ρ=5-10 Ω *cm*; 50 *nm SiO*$_2$, chip sizes: 10x10 *mm*^{2}) by PLD [13].The main advantages of the PLD technique are high flexibility, compatibility with the silicon planar technology, the controlled deposition of multi-component compositions as perovskite oxides in a defined stoichiometry as well as the short deposition time due to the high growth rates. Moreover, the thin-film preparation can be performed in various atmospheres (e.g., O_2, N_2) at elevated temperatures up to 1200°C [12,13]. The BST films were deposited at 400 °C in an oxygen ambient ($2x10^{-3}$ *mbar*) using a KrF excimer laser with a wavelength of 248 *nm*. The laser pulse length, frequency and flounce were 20 *ns*, 10 *Hz*, and 2.5 *J/cm*^{2}, respectively. Before the PLD-growth, a 300 *nm* thick Al film was deposited on the rear side of the chip as a contact layer. For details of PLD process see, e.g. [13].

Fig.1 shows light and SEM pictures of the Mg-doped $Ba_{0.8}$ $Sr_{0.2}$ $Mg_{0.1}Ti_{0.9}O_3$ - SiO2-pSi -SiO_2-Si structure after PLD.

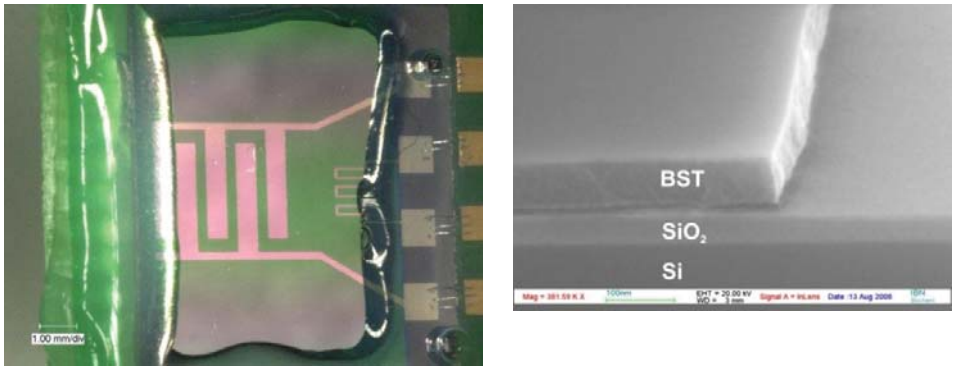

a) b)

Fig. 1. Mg-doped $Ba_{0.8}$ $Sr_{0.2}$ $Mg_{0.1}Ti_{0.9}O_3$ - SiO2-pSi sensor light picture (a) and SEM picture of $Ba_{0.8}$ $Sr_{0.2}$ $Mg_{0.1}Ti_{0.9}O_3$ - SiO2-pSi layer structure after PLD (b) [17]

The prepared perovskite-oxide layers have physically been characterised (thickness, morphology, homogeneity, composition) by means of ellipsometry, atomic force microscopy (AFM) and Rutherford backscattering spectrometry (RBS) methods.

1. ***Ellipsometric spectrometry*[1].** Ellipsometry, as an optical method for determining the film thickness and optical properties, measures the change in the state of polarization of the light reflected off the film's surface. The advancement of spectroscopic ellipsometers has extended the analytical power of ellipsometry to complex multilayer coatings, where several optical parameters (refractive index, extinction coefficient, film thickness, roughness anisotropy, etc) can be determined simultaneously. The enhanced spatial resolution of imaging ellipsometers potentially expands ellipsometry into new areas of microanalysis, microelectronics, and bio-analytics. The results of ellipsometric investigation of the Mg-doped $Ba_{0.8}Sr_{0.2}Mg_{0.1}Ti_{0.9}O_3$ thin film are presented in Fig. 2.

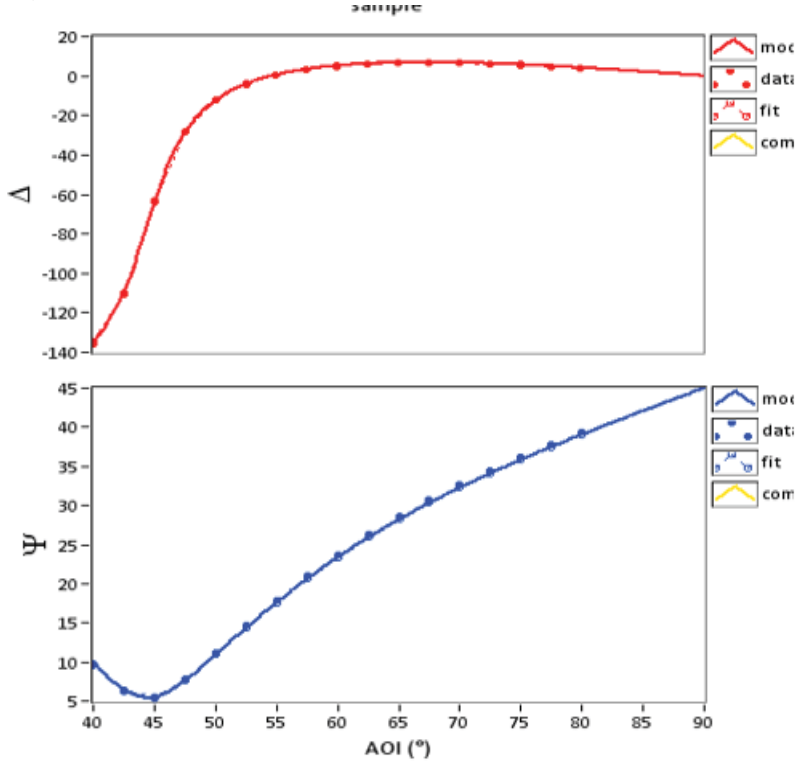

Fig. 2. Ellipsometric measurement results

The investigation and comparison of Mg-doped $Ba_{0.8}Sr_{0.2}Mg_{0.1}Ti_{0.9}O_3$ **targets** prepared by SHS technology [13,17] show that BST thin films behave differently than

[1] **Ellipsometric,** AFM, RBS measurements shown in this work were carried out in Forschungszentrum Juleich and Institute of Bio- and Nanotechnology (Germany).

bulk BST.The dielectric constant of BST thin film is much smaller than bulk BST. It is observed that the dielectric constant decreases with a decrease in the thickness of the BST thin film. The thickness dependence of the dielectric constant varies with the substrate temperature and the grain size effect. The thickness dependence of permittivity is explained in Schottky barrier model [1,2,4].

2. ***Rutherford backscattering spectrometry***. Rutherford backscattering spectrometry (RBS) is a technique for determining stoichiometry, layer thickness, interface quality and crystalline perfection of a thin film. In RBS, the sample is placed in front of a collimated beam of mono-energetic, low mass ions. Within this work, the experiments were performed with 1.4 *MeV* He^+ ions. A small fraction of the ions that impinge on the sample are scattered back elastically by the nuclei of the atoms and are collected by a detector. The detector determines the energy of the backscattered ions, resulting in a energy spectrum - the so-called RBS spectrum.

results	best fit	+/-	unit
Thickness (layer #1@sample)	14,4	0.0	nm
Thickness (layer # 0@sample)	63,7	0.0	nm
RMSE	0,525		

In the *random* configuration (Fig. 3 left side) the sample is rotated to avoid the channeling of the He^+ beam. The energy transferred from a He^+ ion to the sample atom depends on the kinetic energy of the incident ion and the mass of the stationary sample atom. Energy loss, due to inelastic scattering by the electronic structure of the sample atoms, occurs for He^+ ions that penetrate deeper inside the sample. The energy of the ions collected in the detector, thus, provides information about the mass of sample atoms and the thickness of layers. In addition, information about the interface sharpness between two layers is obtained from the abruptness of the low energy edge of the energy interval for the respective sample atoms. Stoichiometry and layer thickness are obtained from the comparison of the so-called *random spectrum* (Fig. 3) with a simulation provided by the program RUMP [18].

The *channeling spectrum* is recorded without rotating the sample during the measurement (Fig. 4). Here, the sample is aligned to a low index crystal direction, allowing the beam to be guided by the atomic rows leading to a reduction of the probability of being backscattered. Defects inside the film will lead to scattering out of the *channeling* direction and a fraction of these ions will be backscattered and collected by the detector. A measure of the crystalline perfection of the sample is, therefore, the minimum yield χ_{min}. This is the minimum in the intensity ratio of *channeling* and *random spectra*.

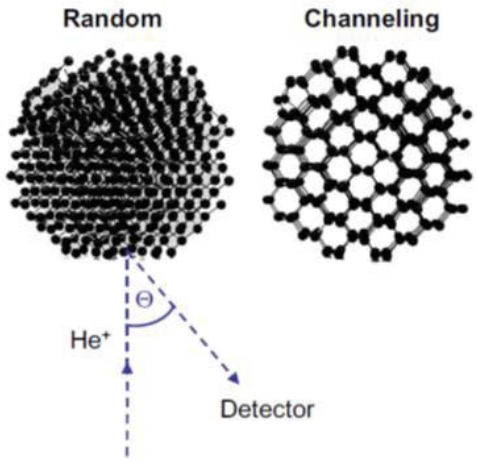

Fig. 3. Shows RBS spectra and channeling measurements

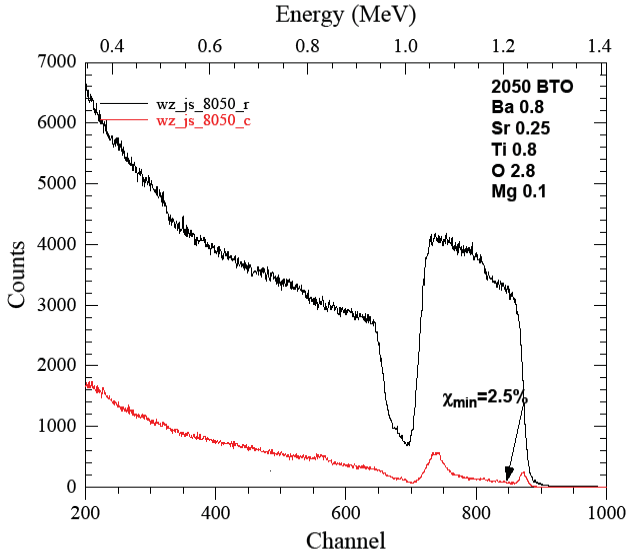

Fig. 4. RBS channeling measurements performed on 63 nm thick $Ba_{0.8}Sr_{0.2}Mg_{0.1}Ti_{0.9}O_3$ film grown on SiO_2 substrate

Clear steps corresponding to the constituent elements (Ba,Sr,Ti,O) were detected. The analysis of the RBS measurement verifies the stoichiometric composition to the deposited $Ba_{0.8}Sr_{0.2}Mg_{0.1}Ti_{0.9}O_3$.

3. ***Atomic force microscopy study.*** Scanning probe microscopy(SPM) is a fast technique that allows the surface analysis of thin films and single crystals with atomic

resolution. The scanning probe technique used in this work is the atomic force microscopy (AFM). AFM measurements were performed on an area 10x10 μm^2 to investigate the surface roughness. The results of the AFM study are illustrated in Fig. 5. They were recorded in the tapping mode using a BioMat Workstation (JPK Instruments, Germany).

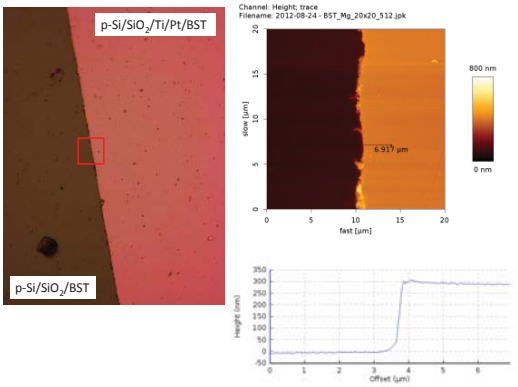

a)

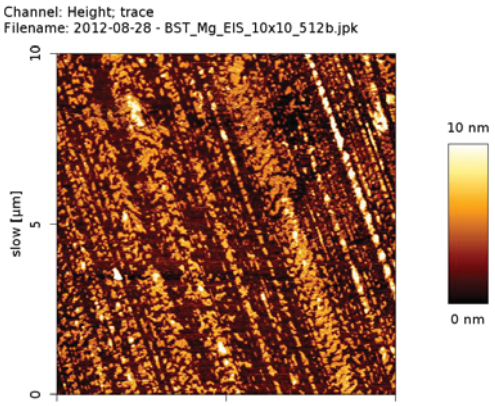

b)

Fig. 5. AFM spectroscopy of $Ba_{0.8}Sr_{0.2}Mg_{0.1}Ti_{0.9}O_3$ thin film. [(a)-surface and height resolution, (b)-high-resolution two dimensional surface image with of the interfacial defects of film]

Conclusions. The results of the ellipsometric investigation of the Mg-doped $Ba_{0.8}Sr_{0.2}Mg_{0.1}Ti_{0.9}O_3$ thin film and the comparison of Mg-doped $Ba_{0.8}Sr_{0.2}Mg_{0.1}Ti_{0.9}O_3$ **targets** prepared by SHS technology [13,17] show that BST thin films behave differ-

ently than the bulk BST. The dielectric constant of the BST thin film is much smaller than that of the bulk BST. It is observed that dielectric constant decreases with a decrease in the thickness of the BST thin film. The thickness dependence of the dielectric constant varies with the substrate temperature and the grain size effect. The thickness dependence of permittivity is explained by Schottky barrier model [1,2,4]. As it follows from Fig. 4, the minimum yield value of 2.5% measured at the Ba-signal reveals the excellent crystalline quality of these films and confirm a stoichiometric good growth. The measured root mean square (rms) roughness is about 7,6 *nm*. The defect can be recognized by a local lattice expansion. A double row of dots of about equal contrast is found corresponding to BaO, SrO columns, meeting each other as denoted by a pair of black arrows.

It is thus likely that decomposition takes place during the exposure to the higher-temperature and lower oxygen pressure conditions in the PLD chamber. The micrographs show a closed BST thin film without micro-cracks or pores. The BST surface possesses a grainy texture with a typical grain size of ~50 *nm*.

References

1. Ferroelectric Materials for Microwave Tunable applications / **A.K. Tagantsev, V.O. Sherman, K.F. Astafiev,** et al // J. of Electroceramics. - 2003. -P.11-66.
2. **Tagantsev A.K. and Gerra G.** Interface-induced phenomena in polarization response of ferroelectric thin films // J. Appl. Phys.- 2006. -100. - P052607-1-28.
3. **Poghossian A., Schöning M.J.** Silicon-Based Chemical and Biological Field-Effect Sensors // Encyclopedia of Sensors / Edit. by C.A. Grimes, E.C. Dickey, and M.V. Pishko. - 2006. – 9.- P.463-533.
4. **Gevorgian S. and Vorobiev A.** Dc field and temperature dependent acoustic resonances in parallel-plate capacitors based on $SrTiO_3$ and $Ba_{0.25}Si_{0.75}TiO_3$ films: Experiment and modelling // J. of Appl. Phys.- 2006.- 99.-P.124112-1-11.
5. Ferroelectric thin films: review of materials, properties, and applications / **N. Setter, D. Damjanovic, L. Eng,** et al // J. Appl. Phys.- 2006.-100.- P.051606-66.
6. **Skinner S. J.** Recent advances in perovskite-type materials for SOFC cathods // Fuel Cells Bull. – 2001.- V.4. - P. 6-12.
7. **Muralt P.** Ferroelectric thin films for micro-sensors and actuators: review // J. Micromech. Microeng. – 2000. – V. 10. - P. 136–146.
8. CO/HC sensors based on thin films of $LaCoO_3$ and $La_{0.8}Sr_{0.2}CoO_3$ metal oxides/ **Brosha, R. Mukundan, D.R. Brown,** et al // Sens. Actuators B.- 2000. - 69. – P. 171-182.
9. **Tofan C., Kirchnerova D.** Decomposition of nitric oxide over perovskite oxide catalysts: effect of Co2, H2o and CH4 // Appl. Catal.-2002.- B36.- P.311-323.
10. **Agarwal S., Samanta S.B., Shara G.L.** Influence of pH on structural and electrical properties of sol-gel derived $(Ba,Sr)TiO_3$ thin films under humid conditions //Thin Solid Films. – 2004.- V.447-448.- P.502-508.

11. A high performance ethanol sensor based on field-effect transistor using a $LaFeO_3$ nanocrystalline thin-film as a gate electrode / **S. Zhao, J.K.O. Sin, B. Xu,** et al // Sens. Actuators. – 2000.- B44. - P.83-87.
12. **Anh D.T.V., Olthuis W., Bergveld P.** Sensing properties of perovskite oxide $La_{0.5}Sr_{0.5}CoO_3$ obtained by using pulsed laser deposition // Sens. Actuators. - 2004. - B 103.- P.165-168.
13. pH-sensitive properties of barium strontium titanate (BST) thin films prepared by pulsed laser deposition technique / **V.V. Buniatyan, N.W. Martirosyan, M.H. Abouzar,** et al // Phys. Status Solidi.-2010.- A 207.- P. 824–830.
14. **Xu S., Qu Y. and Zhang C.** Effect of Mg^{2+} content on the dielectric properties of $Ba_{0.65-x}Sr_{0.35}Mg_xTiO_3$ ceramics // J. Appl. Phys.- 2009.- 106. - P. 014107-1-5.
15. **Lin T.N., Chu J.P., Wang S.F.** Structures and properties of Ba0.3Sr0.7TiO3: MgTiO3 ceramic composites // Materials Letters. – 2005.- 59. - P.2786 - 2789.
16. **Li Z.C. and Bergman B.** Electrical properties and ageing characteristics of $BaTiO_3$ ceramics doped by single dopants // Journal of the European Ceramic Society. - 2005. - 25.- P. 441-445.
17. **Araghi M.A.K.** Self propagating high-temperature synthesis Mg–doped barium-stronyium titanate // Bull. Collection of Scientific papers, SEUA .- 2012.- P.1.- P. 396-401.
18. **Doolittle L.R.** Asemiautomatic algorithm for Rutherford backscattering analysis // Nucl. Instrum. Meth. - 1989.- B15. - P.227–231.

Received on 10.09.2017.
Accepted for publication on 21.12.2017.

ՖԵՐՈԷԼԵԿՏՐԱԿԱՆ ՆՈՒՐԲ ԹԱՂԱՆԹՆԵՐԻ ՖԻԶԻԿԱԿԱՆ ԲՆՈՒԹԱԳՐՈՒՄԸ

Վ.Վ. Բունիաթյան, Խալիլի Արաղի Ալի Մոհամմադ, Ա.Ա. Դավթյան

Ներկայացվել են Mg-ով լեգիրված $Ba_{0.8}Sr_{0.2}Mg_{0.1}Ti_{0.9}O_3$ ֆերոէլեկտրական նուրբ թաղանթների ֆիզիկական ու կառուցվածքային բնութագրման արդյունքները: $(Ba,Sr)<Mg>TiO_3$ կերամիկական թիրախները ստացվել են ինքնատարածվող բարձրջերմաստիճանային սինթեզի (ԻԲՍ), իսկ նուրբ թաղանթները՝ իմպուլսային լազերային փոշեցրման (ԻԼՓ) մեթոդներով: Ֆերոէլեկտրական թաղանթները բնութագրվել են ֆիզիկական (հաստություն, մակերևութային խորդուբորդություններ, բաղադրություն) բնութագրիչներով էլիպսամետրական, տեսածրող էլեկտրոնային մանրազննման (ՏԷՄ), ատոմաուժային մանրազննման (ԱՈՒՄ) և Ռուդերֆորդի հակաանդրադարձային սպեկտրասկոպիական (ՌՀՍ) մեթոդներով: Mg-ով լեգիրված $Ba_{0.8}Sr_{0.2}Mg_{0.1}Ti_{0.9}O_3$ նուրբ թաղանթների էլիպսաչափական հետազոտությունները և դրանց համեմատությունը Mg-ով լեգիրված $Ba_{0.8}Sr_{0.2}Mg_{0.1}Ti_{0.9}O_3$ թիրախների հետ, որոնք պատրաստվել են ԻԲՍ մեթոդով, ցույց են տվել, որ BST նուրբ թաղանթի և թիրախի վարքերը էականորոն տարբերվում են: Նկատվել է, որ դիէլեկտրիկական հաստատունը նվազում է BST թաղանթի հաստության նվազմանը զուգընթաց: Թաղանթի հաստությունից դիէլեկտրիկական թափանցելիության

կախվածությունը փոփոխվում է հարթակի ջերմաստիճանից, ինչպես նաև հատիկներում չափային երևույթների հետևանքով: Դիէլեկտրիկական թափանցելիության՝ հաստությունից կախվածությունը բացատրվում է Շոտկիի արգելքի մոդելով: Քննարկվող նմուշների ՌՀՄ հետազոտությունները հավաստում են գերազանց բյուրեղային ստիխիոմետրական և բյուրեղի լավ որակի աճեցման մասին: Խորդուբորդությունների միջինքառակուսային մեծությունը կազմում է ~7,6 *նմ*: Միկրոնկարը վկայում է BST թաղանթի առանց միկրոճեղքերի և ծակոտկենության առկայությունը: BST թաղանթն օժտված է ~50 *նմ* տիպական չափսերով հատիկայնությամբ:

Առանցքային բառեր. բարիում-ստրոնցիում տիտանատ, էլիպսաչափություն, ատոմաուժային մանրազննում:

ФИЗИЧЕСКАЯ ХАРАКТЕРИЗАЦИЯ ФЕРРОЭЛЕКТРИЧЕСКИХ ТОНКИХ ПЛЕНОК

В.В. Буниатян, Халили Арахи Али Могаммад, А.А. Давтян

Представлены результаты физических и структурных характеризаций Mg–легированных $Ba_{0.8}Sr_{0.2}Mg_{0.1}Ti_{0.9}O_3$ тонких пленок. Керамические мишени (Ba,Sr)<Mg>TiO_3 получены методом самораспространяющегося высокотемпературного синтеза (СВС), а тонкие пленки – методом импульсного лазерного распыления (ИЛР). Ферроэлектрические пленки физически (толщина, поверхностная неравномерность, композиция) характеризуются эллипсометрическим, сканирующим электронным микроскопическим (СЭМ), атомно–силовым микроскопическим (АСМ) методами и антирефлекторной спектроскопией Рудерфорда (АСР). Результаты эллипсометрических исследований Mg-легированных $Ba_{0.8}Sr_{0.2}Mg_{0.1}Ti_{0.9}O_3$ тонких пленок и их сравнение с Mg-легированными $Ba_{0.8}Sr_{0.2}Mg_{0.1}Ti_{0.9}O_3$ мишенями, полученными технологией СВС, показывают, что поведение BST тонких пленок и мишени отличается. Зафиксировано, что диэлектрическая постоянная уменьшается с уменьшением толщины тонких пленок BST. Характер связи диэлектрической постоянной и толщины изменяется в зависимости от температуры подложки и размерных зернистостных эффектов. Зависимость диэлектрической постоянной от толщины объясняется с помощью модели барьера Шоттки. Исследование тонких пленок BST РАС показывает стихиометрическое совпадение и свидетельствует о наличии отличной кристаллической структуры и хорошем качестве выращивания кристаллических пленок. Измеряемая среднеквадратичная неравномерность поверхности составляет ~ 7,6 *нм*. Микрорисунки BST тонких пленок свидетельствуют об отсутствии микротрещин и пористостей. Поверхность BST является неравномерной с типичными размерами ~50 *нм*.

Ключевые слова: титанат бария–стронция, эллипсометрия, атомно-силовая микроскопия.